

Low-density, one dimensional quantum gases in the presence of a localised attractive potential

J. Goold, D. O'Donoghue, and Th. Busch

E-mail: jgoold@phys.ucc.ie

Department of Physics, National University of Ireland, UCC, Cork, Ireland

Abstract. We investigate low-density, quantum-degenerate gases in the presence of a localised attractive potential in the centre of a one-dimensional harmonic trap. The attractive potential is modelled using a parameterised δ -function, allowing us to determine all single particle eigenfunctions analytically. From these we calculate the ground state many-body properties for a system of spin-polarised fermions and, using the Bose-Fermi mapping theorem, extend the results to strongly interacting bosonic systems. We discuss the single particle densities, the pair correlation functions, the reduced single particle density matrices and the momentum distributions as a function of particle number and strength of the attractive point potential. As an important experimental observable, we place special emphasis on spatial coherence properties of such samples.

PACS numbers: 03.75.Gg, 03.65.Ge, 37.10.De, 05.30.Jp

1. Introduction

The rapid advances made in the fields of atom cooling and trapping have created renewed theoretical and experimental interest into lower-dimensional systems [1, 2, 3, 4, 5, 6, 7]. Even though restricting the spatial degrees of freedom often leads to stronger correlation, various exactly solvable models are known that cover different temperature and interaction regimes. One example of this is the Lieb-Liniger gas [8, 9], a model for a quantum gas of bosons trapped in one dimension and interacting via a point-like potential. Using the Bethe ansatz [10], this model can be exactly solved and it was realised by Girardeau [11] that in the limit of infinitely strong repulsive interactions a particularly elegant solution can be found by mapping it onto a gas of free fermions.

This strongly correlated limit of the Lieb-Liniger model is known as the Tonks-Girardeau (TG) gas [11, 12] and the first examples for which it was solved were free space and box-like systems with periodic boundary conditions [11, 13]. Recently quantum gases in the TG limit were experimentally realised [14, 15] and used to observe non-equilibrium dynamics [16]. In anticipation and in light of the experimental realisation Wright and Girardeau managed to extend the number of exactly known solutions by describing the gas subject to a harmonic trap [17, 18] and several other authors have considered a range of different potentials [19, 20, 21, 22, 23]. In this work we extend the recent progress and explore the ground state properties of a TG gas (and by means of the mapping theorem also of a gas of non-interacting, spin-polarised fermions) in a harmonic trap in the presence of a localised attractive potential at the trap centre. We place particular emphasis on spatial coherence effects.

Even though a description for solving the TG gas analytically exists it is often still necessary to involve numerical calculations, especially if a larger number of particles is considered. While these can be time and resource consuming, approximations have been found recently to investigate ground state properties of samples with large particle numbers [24, 25]. For mesoscopic samples an algorithm allowing efficient calculation of the reduced single particle density matrix (RSPDM) for a TG gas in an arbitrary potential was recently presented by Pezer *et al.* [26]. As many of the important groundstate properties of a many-body systems can be directly calculated from a system's reduced single particle density matrix we will employ this algorithm in this work.

Localised, attractive potentials have recently been used with and suggested for several experiments within ultracold quantum gases. Highly focussed optical beams were shown to allow an increase in the phase-space density of a gas and drive its transition towards Bose-Einstein condensation [27, 28]. Uncu *et al.* have shown that such processes can be analysed using point-like functions [29, 30]. A second way of creating a highly localised potential is given by trapping an impurity inside a cloud of cold atoms. For ions, for example, the trapping frequencies can be several 100 kHz and they therefore provide very localised potentials [31]. The harmonic trap with a point like potential at the center as considered in this work is a well fitting toy model for such a situation.

In order to find the many-body solutions in a given geometry for the TG gas (or for non-interacting fermions) one must know the exact single particle eigenstates. This is a problem in itself, as the list of exactly solvable single particle problems in quantum mechanics is limited. The system we consider here is the harmonic trap with a point-like potential trapped at its centre. For a repulsive potential this resembles the limit of a double well trap and was recently investigated for boson as well as fermionic systems [19, 22]. The groundstate physics for the same potential of a bosonic pair, up to and including the Tonks regime, was also rigorously analyzed [32]. Here we describe the systems properties for the other limit, i.e. for a trap with an attractive central δ -potential. It is important to emphasize that this is a setting very different to the repulsive case as the attractive potential possesses an additional bound state.

Through the Fermi-Bose mapping theorem the bosonic wave-function can be calculated directly from the appropriately chosen fermionic one by symmetrization. Since the symmetry or antisymmetry of a wave function does not have an influence on the density distribution, the spatial density profiles for fermionic and bosonic samples in this limit are indistinguishable. Therefore, whenever results concerning density distributions are presented in this paper, they apply to fermionic as well as to bosonic samples.

The paper is organised as follows: in Sec. 2 we define the many-body Hamiltonian for our system and briefly describe the technique to solve it for non-interacting fermions as well as for hard-core bosons. In Sec. 3 we review the single particle eigenspectrum of the the harmonic trap with a central attractive δ -function and in Sec. 4 we calculate the many-body groundstate properties of a TG gas in such a potential. The corresponding results for free fermions are also shown. Special emphasis is put on spatial coherence effects. Finally we conclude in Sec. 5.

2. Model Hamiltonian

We consider a gas of N identical atoms trapped in a tight atomic waveguide, such that the dynamic of the gas is strongly restricted in the transversal directions. In the low-temperature limit this allows us to choose a one-dimensional model where the parameterisation of the scattering interaction takes the three dimensional nature of the particles into account [33]. In the remaining direction we then consider a harmonic potential perturbed in the center by a well localised attractive potential, which we model by a parameterised δ -function. For sufficiently low density we only need to consider two-particle collisions and the Hamiltonian can be written as

$$\mathcal{H} = \sum_{n=1}^N \left(-\frac{\hbar^2}{2m} \frac{\partial^2}{\partial x^2} + \frac{1}{2} m \omega^2 x_n^2 - \kappa \delta(x_n) \right) + \sum_{i < j} V(|x_i - x_j|), \quad (1)$$

where m is the mass of a single atoms, ω the frequency of the harmonic potential and κ the strength of the point-like attractive potential, which is located at $x_n = 0$. The particle-particle interaction potential depends only on the relative distance between two particles.

For purposes of clarity and readability we re-scale the above Hamiltonian to harmonic oscillator units where all length are in units of the ground state size, $a_0 = \sqrt{\hbar/m\omega}$, and all energies in terms of the oscillator energy, $\hbar\omega$,

$$\bar{\mathcal{H}} = \sum_{n=1}^N \left(-\frac{1}{2} \frac{\partial^2}{\partial \bar{x}^2} + \frac{1}{2} \bar{x}_n^2 - \bar{\kappa} \delta(\bar{x}_n) \right) + \sum_{i < j} V(|\bar{x}_i - \bar{x}_j|) . \quad (2)$$

This leads to a new scaled strength for the attractive potential given by $\bar{\kappa} = (\hbar\omega a_0)^{-1} \kappa$. For notational simplicity we shall drop the overbars on all scaled quantities and acknowledge that we are, henceforth, dealing in the scaled units just described. All units used in calculations and figure plots in this paper are in terms of these scaled units.

2.1. Fermions

In order to avoid any confusion we first consider the interaction term in the bosonic and fermionic cases separately. Fermionic systems can be analyzed by realizing that due to the antisymmetric nature of the wave-function no s -wave scattering between two particles can happen. As p -wave scattering at low temperature is negligible (unless close to a resonance), the Hamiltonian (1) can be approximated by neglecting any inter-particle scattering and solving the problem for free particles.

2.2. Bosons

For bosonic systems at low temperatures the atomic interaction potential can be well approximated by a point-like potential, $V(|x_i - x_j|) = g_{1D} \delta(|x_i - x_j|)$. This approximation is frequently used and the only reminiscence of the exact potential is given by the three-dimensional s -wave scattering length, a_{3D} [34]. For positive values of a_{3D} the interaction is repulsive and for negative values it is attractive. This scattering length is then related to the one-dimensional coupling constant via

$$g_{1D} = \frac{4\hbar^2 a_{3D}}{ma_{\perp}} (a_{\perp} - Ca_{3D})^{-1} , \quad (3)$$

where C is a constant of value $C = 1.4603 \dots$ [33]. In this work we will purely focus on very strong repulsively interacting systems, which in low dimensions corresponds to the low density limit and is known as the Tonks-Girardeau limit.

One of the remarkable features of this limit is that it becomes exactly solvable using the so-called Fermi-Bose mapping theorem. The theorem follows from replacing the interaction term in the Hamiltonian in eq. (2) with the following constraint on the allowed wave-functions

$$\Psi = 0 \quad \text{if} \quad |x_i - x_j| = 0, \quad i \neq j \quad (1 \leq i \leq j \leq N) , \quad (4)$$

which is equivalent to the demands of the Pauli-exclusion principle for a gas of spinless fermions. One can therefore compute the many-body bosonic ground-state wave-function from the fermionic case, using the simple symmetrization

$$\Psi_B(x_1, \dots, x_N) = |\Psi_F(x_1, \dots, x_N)| . \quad (5)$$

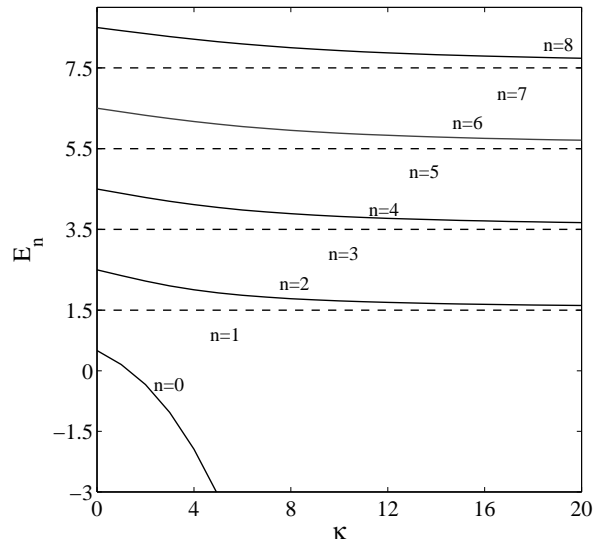


Figure 1. Single particle energy eigenspectrum for the harmonic trap with an attractive point potential at the trap center. The solid curves correspond to the symmetric eigenstates and the broken lines to the anti-symmetric eigenstates. Note the existence of the trapped eigenstate originating from the attractive point-potential.

This procedure transforms the strongly interacting bosonic problem into a problem treating non interacting fermions. As for non-interacting fermions calculation tools are known, the problem becomes treatable.

Therefore the bosonic as well as the fermionic problem can be solved if the single particle problem can be solved. If this solution is even analytic, no further approximations to the many-particle wave-function have to be made.

3. Eigenstates of the harmonic trap with central attractive point potential

Even though the eigenstates of a harmonic trap with a central attractive δ -potential are well known [35], we will briefly review them in this section. It is easy to see that owing to its point-like nature all eigenenergies associated with odd eigenstates of an undisturbed harmonic oscillator are independent of the strength of the δ -function. All energies associated with the even eigenstates, on the other hand, will decrease non-trivially with increasing values of κ . And while all excited even eigenstates are bound from below by the energies of the next, lower lying odd eigenstate, the energy of the ground state E_0 becomes unbounded from below in the $\kappa \rightarrow \infty$ limit (see Fig. 1). This is due to the existence of a bound state within the attractive point potential which is accessed by the system once the ground state energy $E_0 < 0$, which corresponds to $\kappa = 0.675978$. The even eigenstates are then given by

$$\psi_n(x) = \mathcal{N}_n e^{-\frac{x^2}{2}} U\left(\frac{1}{4} - \frac{E_n}{2}, \frac{1}{2}, x^2\right) \quad n = 0, 2, 4 \dots, \quad (6)$$

where \mathcal{N}_n is the normalization constant and $U(a, b, z)$ are the Kummer functions [36]. The corresponding eigenenergies, E_n , are determined by the roots of the implicit relation,

$$\kappa = 2 \frac{\Gamma\left(-\frac{E_n}{2} + \frac{3}{4}\right)}{\Gamma\left(-\frac{E_n}{2} + \frac{1}{4}\right)}. \quad (7)$$

By contrast, the antisymmetric eigenfunctions vanish at the origin and are unaffected by the point potential. They are therefore given by the odd eigenstates of the unperturbed harmonic potential ($\kappa = 0$)

$$\psi_n(x) = \mathcal{N}_n H_n(x) e^{-\frac{x^2}{2}} \quad n = 1, 3, 5 \dots, \quad (8)$$

where $H_n(x)$ is the n^{th} order Hermite polynomial. The corresponding energies are given by the eigenvalues of the odd parity states of the harmonic oscillator, $E_n = \left(n + \frac{1}{2}\right)$. Since we know the single particle eigenstates, we can build the Slater determinant for the problem of non-interacting fermions and through the symmetrisation of the mapping theorem we can calculate the exact many-body bosonic wave-function.

4. Ground-state properties

4.1. Single-particle densities and pair-distribution functions

The single particle density for the bosonic as well as the fermionic system is defined as

$$\rho(x) = N \int_{-\infty}^{+\infty} |\Psi_B(x, x_2 \dots, x_N)|^2 dx_2 \dots dx_N = \sum_{n=0}^{N-1} |\psi_n(x)|^2. \quad (9)$$

In Fig. 2 we show $\rho(x)$ for a gas of 20 particles for three different values of κ . The introduction of the attractive point potential to the harmonic trap results in the emergence of a central density spike, which grows quasi-linearly with increasing strength of the attractive potential (see Fig. 2, right most figure). This feature originates from the strongly localised nature of the bound state of the δ -function and, which is also the reason for the potential having virtually no influence on the overall width of the density distribution.

The pair-distribution function, $D(x_1, x_2)$, is a two particle correlation function that describes the probability to measure two different particles at two given positions at the same time. It is defined in the following way

$$D(x_1, x_2) = N(N-1) \int_{-\infty}^{+\infty} |\Psi_B(x_1, x_2 \dots, x_N)|^2 dx_3 \dots dx_N, \quad (10)$$

$$= \sum_{0 \leq n \leq n' \leq N-1}^{N-1} |\psi_n(x_1)\psi_{n'}(x_2) - \psi_n(x_2)\psi_{n'}(x_1)|^2, \quad (11)$$

and in Fig. 3 we show its evolution for a sample of 20 particles under increasing strength of the point potential. Most notably, in the $\kappa = 0$ case we notice the absence of any probability along the line $x_1 = x_2$, which is due to the strong repulsion between the particles. Secondly, with increasing κ a cross type pattern of high probability density

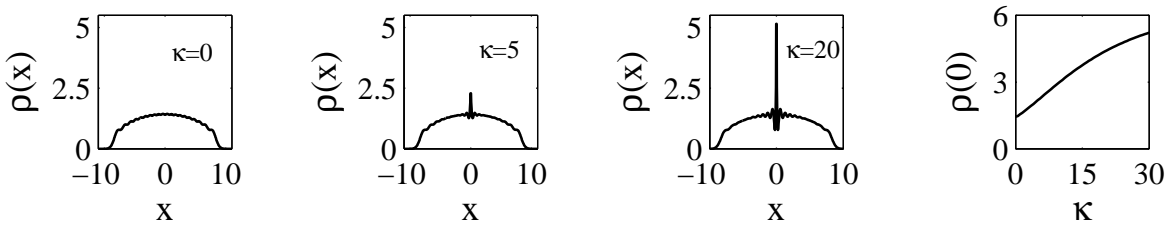


Figure 2. The first three plots from left to right show the single particle densities $\rho(x)$ for 20 particles and for different values of the potential strengths $\kappa = 0, 5$ and 20. As the attractive potential is assumed to be point-like, it has no significant influence on the size of the atomic cloud and only introduces a very localised disturbance. The height of the central disturbance, $\rho(0)$, is shown as a function of κ in the right-most plot.

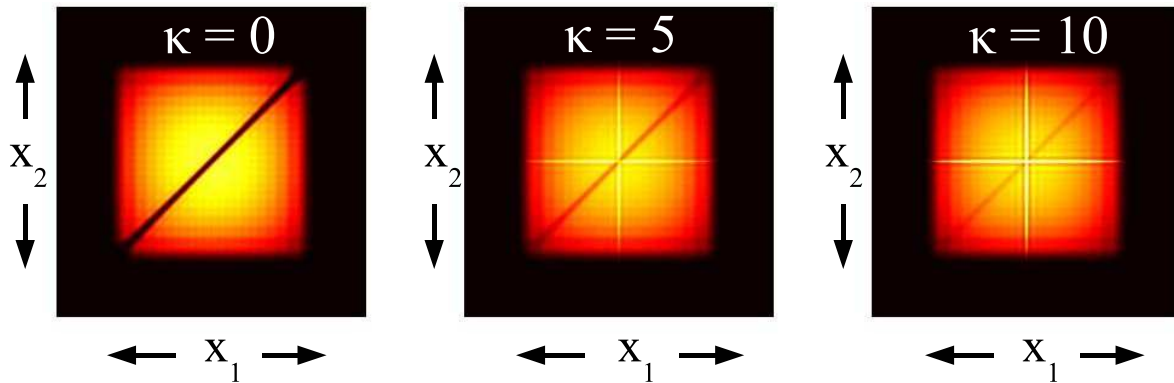


Figure 3. Pair-distribution function $D(x_1, x_2)$ for $N = 20$ particles and potential strengths $\kappa = 0, 5$, and 10. Each plot spans the range $-10 < x_1, x_2 < 10$. The manifestation of the bound state within the attractive potential can be clearly seen in the emergence of a cross of localised probability along the lines $x_1, x_2 = 0$

emerges along the $x_1 = 0$ and $x_2 = 0$ lines. This is in agreement with the appearance of the peak at $x = 0$ in the density plots and corresponds to the lowest eigenstate becoming bound and strongly localized within the point potential. Again, the appearance of the localized disturbance does not have any large influence on the pair distribution function at larger values of x .

4.2. Reduced single particle density matrices and natural orbitals

Although a many-body wave-function fully characterizes a quantum mechanical state, a RSPDM is a useful and convenient tool for deriving many important properties of many-body systems. In particular the expectation values of many important one-body quantities such as the momentum distribution or the von Neumann entropy are easily obtained from it. The RSPDM for a 1-D gas of spinless, non-interacting fermions is

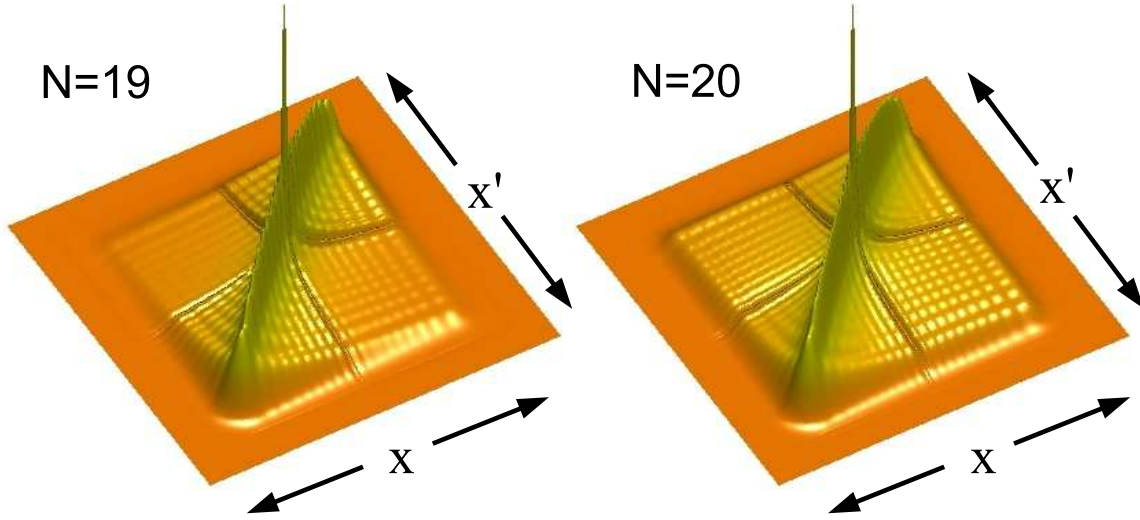


Figure 4. RSPDM $\rho_B(x, x')$ for $N = 19$ and $N = 20$ bosons in a harmonic trap with a central attractive point potential of strength $\kappa = 10$. One notices a distinct difference in the off diagonal behavior for different particle numbers. Each plot spans the range $-10 < x, x' < 10$.

given by

$$\rho_F(x, x') = \sum_{n=1}^N \psi_n(x) \psi_n^*(x'), \quad (12)$$

and is diagonal by default since it is a projector onto an N -dimensional subspace of the Hilbert space of possible one particle states. Although we do not show plots of the matrices here, we will refer to the RSPDM later when we investigate how the momentum distribution of a harmonically trapped Fermi sea is modified by introduction of the attractive point potential.

The RSPDM for the bosonic case is defined as

$$\rho_B(x, x') = \int_{-\infty}^{+\infty} \Psi_0^B(x, x_2, \dots, x_N) \Psi_0^B(x', x_2, \dots, x_N) dx_2 \dots dx_N, \quad (13)$$

and normalized to $\int \rho_B(x, x) dx = N$. Due to the inter-bosonic interactions it is not diagonal in the basis of single particle states and for finite values of κ we will solve for it numerically below. A naive calculation strategy is still a numerical feat due to the large demands on memory space. However, Pezer and Buljan [26] have recently presented an algorithm that allows this calculation to be carried out very effectively and it is this algorithm which we employ here to calculate $\rho_B(x, x')$. Note that for the $\kappa = 0$ case the integral (13) was recently solved analytically [37].

The RSPDM expresses self correlation and one can view $\rho_B(x, x')$ as the probability that, having detected the particle at position x , a second measurement, immediately following the first, will find the particle at the point x' . Classically one would only expect a result for $x = x'$, however quantum mechanically off-diagonal correlations become important. In Fig. 4 we show the RSPDM for an odd ($N = 19$) and an even

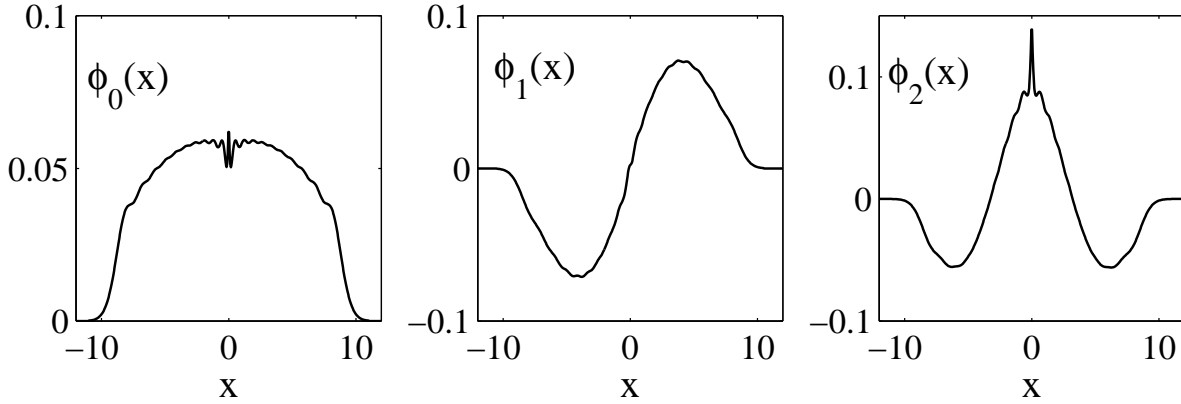


Figure 5. The first three, energetically lowest lying natural orbitals for a Tonks-Girardeau gas of 20 particles in a harmonic trap with an attractive point potential of strength $\kappa = 10$. The influence of the attractive potential on the even states can be clearly seen.

($N = 20$) number of particles in the presence of a strong attractive potential with $\kappa = 10$. In both figures a spike at $x = x' = 0$ is the dominating feature, originating from the bound state within the delta-function and matching with the results for the single particle density (9), which can be obtained from the diagonal $\rho(x) = \rho_B(x, x' = x)$. This localised nature also explains the absence of any probability density in the cross defined by the lines $x = 0, x' = 0$. It is clear from Fig. 4 that there is a distinct difference between systems with odd and even particle numbers. In the $N = 19$ case we see that the probability in the off-diagonal quadrants is strongly depleted as compared to the $N = 20$ system. This effect occurs for all consecutive odd and even particle numbers studied. A similar odd-even effect was observed in the repulsively split trap [22] and later in the split box [23]. Contributions in the off diagonals of the RSPDM mean that the sample has some degree of spatial coherence and we will interpret this effect with respect to physically observable quantities in the next section.

In order to allow for an easier interpretation of the bosonic RSPDM we change to a representation in which the matrix becomes diagonal

$$\int_{-\infty}^{\infty} \rho_B(x, x') \phi_j(x') dx' = \lambda_j \phi_j(x). \quad (14)$$

The eigenfunctions $\phi_j(x)$ are known in theoretical chemistry as 'natural orbitals' and their associated eigenvalues λ_j represent the occupation number of the eigenvector. The first three natural orbitals with lowest energy of a 20 particle harmonically trapped TG gas in the presence of an attractive point potential, $\kappa = 10$, are shown in Fig. 5. One can see that the point potential has a strong, localised influence on the shape of the symmetric orbitals, whereas the antisymmetric orbitals are not affected and retain the same shape as in the $\kappa = 0$ case [18].

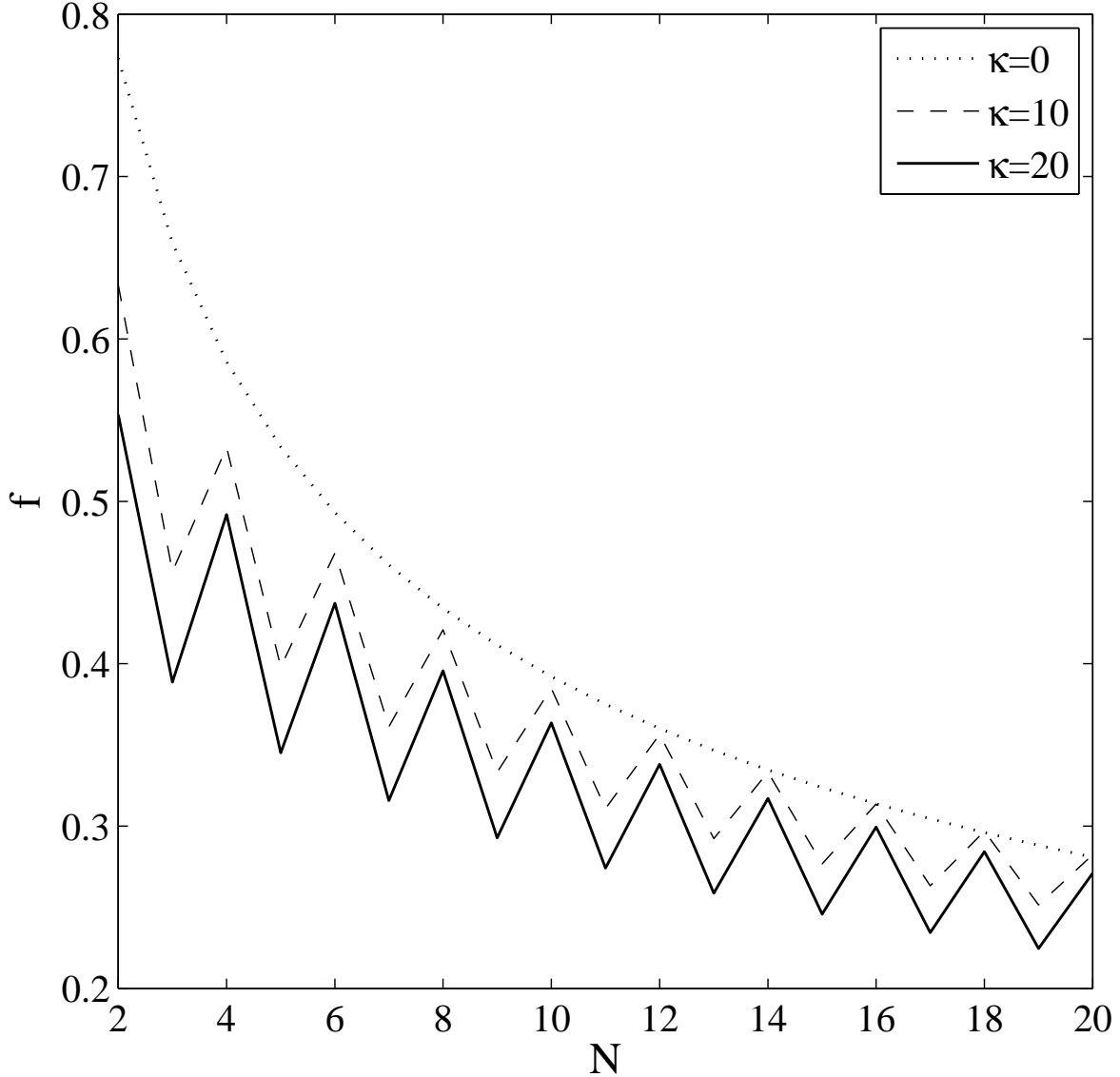


Figure 6. The ground state occupation fraction $f = \frac{\lambda_0}{N}$ as a function of particle number N for the potential strengths $\kappa = 0, 10$ and 20 .

4.3. Ground State Occupation Numbers

The largest macroscopic eigenvalue λ_0 measures the fraction of particles that are in the $\phi_0(x)$ orbital, sometimes known as the 'BEC' state, by $f = \frac{\lambda_0}{N}$. It can hence be used as a measure of the coherence in the system. For the TG gas this was first studied by Girardeau *et al.* for the simple harmonic trap [18] and small particle numbers. They found that despite the strong interactions macroscopic coherence effects can still exist. Later Forrester *et al.* showed that as one increases the particle number, λ_0 tends toward \sqrt{N} [24]. Here we study how increasing the strength of the attractive point-like potential affects this \sqrt{N} behavior.

The groundstate occupation fraction, as a function of N , for the bosonic TG gas

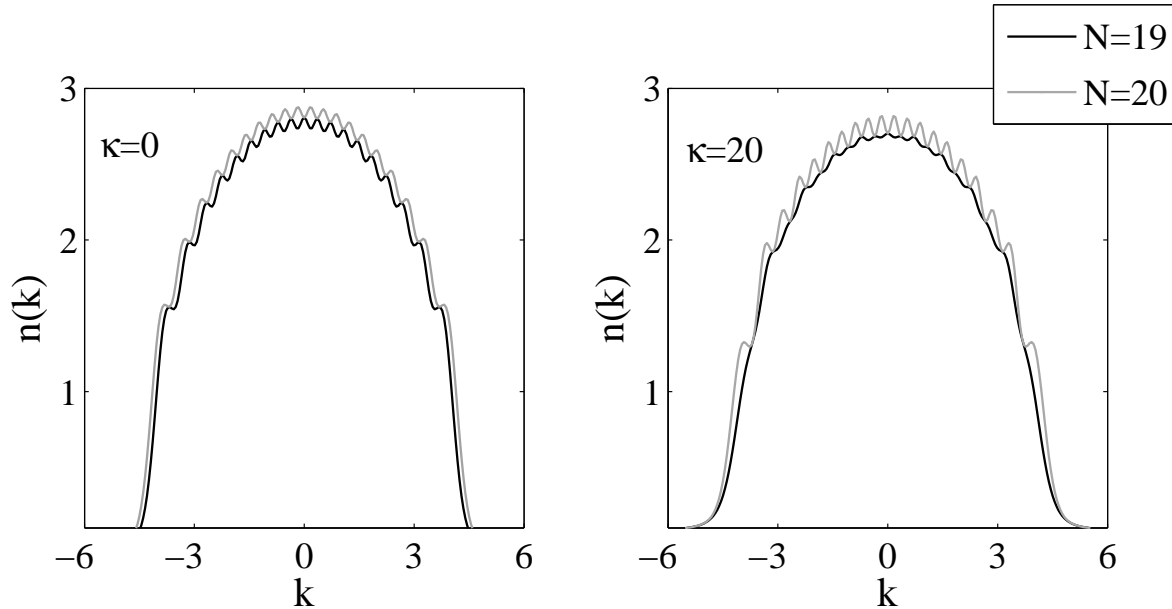


Figure 7. Momentum distributions of a $N = 19$ (black) and a $N = 20$ (grey) particle spin-polarized Fermi gas in a harmonic trap with central attractive point potential. The $\kappa = 0$ and $\kappa = 20$ cases are shown separately.

is shown in Fig. 6 for two different potential strengths and compared to the simple harmonic oscillator result. One can see that the introduction of the central potential creates a distinct, oscillating pattern, which become more pronounced for increased depth. We notice that when the particle number is odd the value of λ_0 or the ‘coherence’ is relatively lower than when the particle number is even. These oscillations in the occupation fraction damp out with increasing number of particles and are similar to an effect recently found for a repulsive δ -barrier [22] (see also [23]). The main difference is a reversal of the oscillations, with the even number samples coherence being decreased stronger in the repulsive case.

This oscillation pattern was identified as being the result of a pairing of single particle energy levels in the repulsive case, which is also the explanation in this situation. While, however, in the case for $\kappa > 0$ consequent even energy levels increased in energy and paired with the next higher lying odd levels, here consequent odd-even levels pair due to a decrease in the energy of the even levels (see Fig. 1). At the same time the remaining ground state is becoming unbounded from below. A more qualitative picture can be given by assuming one-particle to be strongly bound within the δ -potential and acts as a barrier for the remaining $N - 1$ particle system.

Let us in the following investigate how this odd-even coherence effect manifests itself in two experimentally realizable quantities, namely the momentum distribution and interference fringe visibility during free temporal evolution.

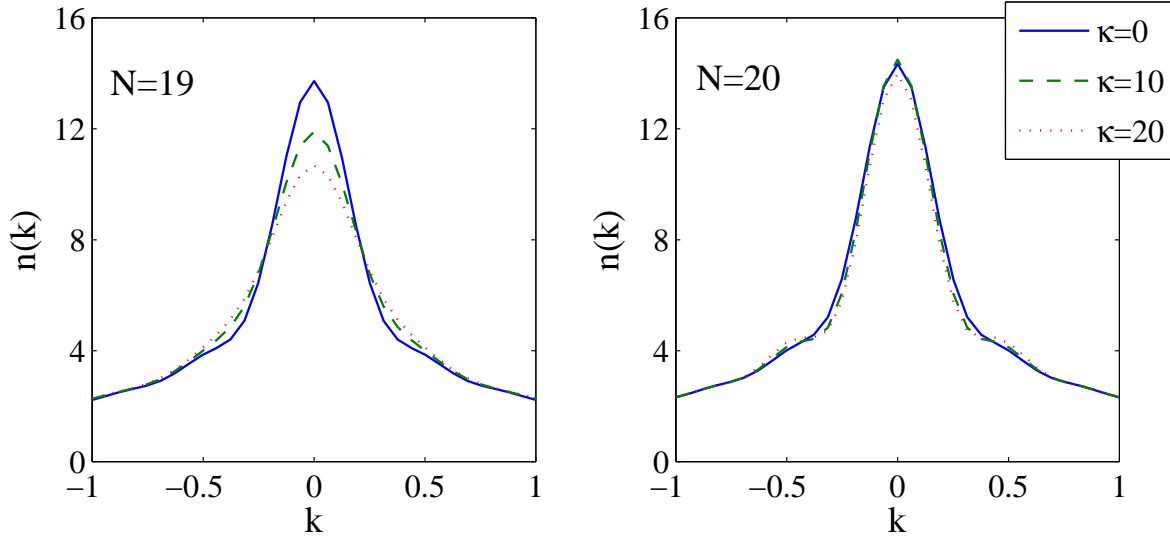


Figure 8. Momentum distribution peak for a $N = 19$ and $N = 20$ particle bosonic TG gas in a harmonic trap with a central attractive point potential of strength $\kappa = 0, 10$ and 20 .

4.4. Momentum Distribution

Although the spatial density profiles are equivalent for a gas of non-interacting fermions and strongly interacting bosons they still show distinctly different momentum distributions

$$n_{B(F)}(k) = (2\pi)^{-1} \int_{-\infty}^{\infty} dx \int_{-\infty}^{\infty} dx' \rho_{B(F)}(x, x') e^{-ik(x-x')}, \quad (15)$$

where the normalization is chosen to be $\int_{-\infty}^{\infty} n(k) dk = N$. Alternatively, the spectral decomposition of $\rho_{B(F)}(x, x')$ allows us to compute the momentum distribution for arbitrary particle number by virtue of

$$n_{B(F)}(k) = \sum_j \lambda_j |\mu_j(k)|^2, \quad (16)$$

where $\mu_j(k)$ are the Fourier transforms of the diagonal basis states. In the special case of free fermions with ρ_F given by eq. (12) these are simply the single particle eigenstates with $\lambda_j = 1$. In Fig. 7 we show the momentum distribution for $N = 19$ and $N = 20$ particles for the potential strengths $\kappa = 0$ and $\kappa = 20$. One can see that for the even particle number the introduction of the central point-potential strongly affects the depth of the oscillations and for the odd particle number setting it has the effect of smoothing them out. In this fermionic case the effect can be attributed to the fact that the point potential introduces non-smooth kinks into the single particle eigenstates which build the Slater determinant.

The momentum distribution of the bosonic case for $N = 19$ and $N = 20$ particles is shown in Fig. 8. One can see that for the odd number sample the δ -potential has the effect of lowering the peak of the distribution, indicating a loss of coherence in agreement

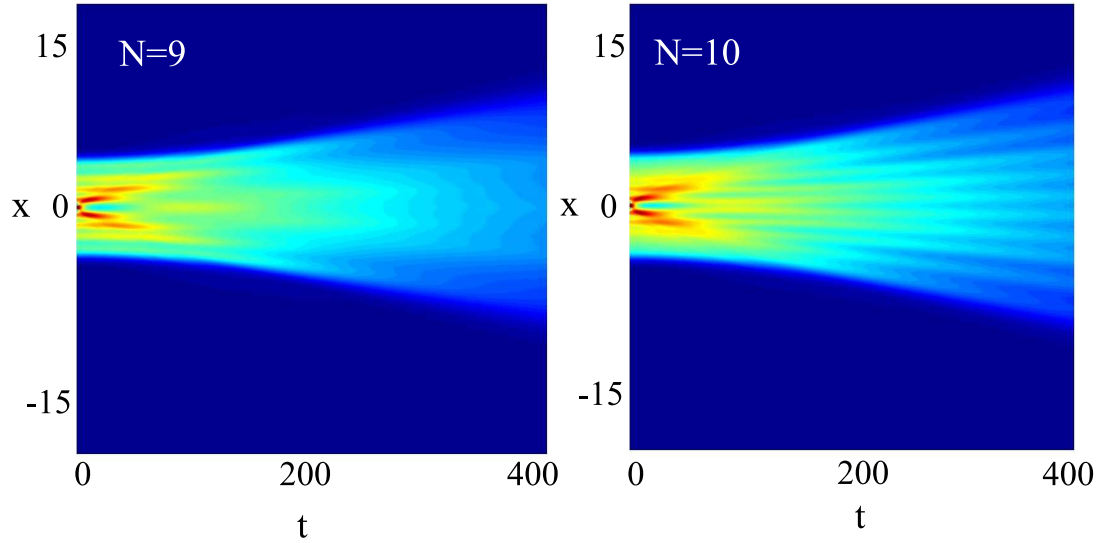


Figure 9. Free space time evolution of the single particle density for a bosonic TG gas consisting of $N = 9$ (left) and $N = 10$ (right) particles initially in trap with an attractive potential of strength $\kappa = 30$. Due to the Fermi-Bose mapping the simulations apply equally well to fermions.

with Fig. 6. For the $N = 20$ plot one can see the appearance of bi-modality through the introduction of the attractive point-potential. This can be interpreted this as single particle interference arising from the fact that one particle is *unpaired* and therefore spatially de-localised over both sides of the split trap by the point potential.

4.5. Interference Patterns

The Fermi-Bose mapping theorem is also applicable to time dependent wave-functions dynamics and in this section we will study the time evolution of the many-body quantum state after removal of all external potentials. To do this we first find the ground state for the sample initially confined to the harmonic trap with a central strong attractive point potential. We then calculate the time evolution of this state as both, the trap and the central splitting, are turned off and the gas undergoes free temporal evolution. During this particles in both halves of the trap will start overlapping and interfering. The single particle densities for two samples with odd ($N = 9$) and even ($N = 10$) particle number are shown in Fig. 9. It is clearly noticeable that the fringe visibility in the even case is much higher than in the odd case, where there is virtually none. This again is a consequence of the larger coherence associated with an even particle number and is consistent with the results in previous sections. As we are describing spatial densities here, this effect is also present in a non-interacting fermion gas.

5. Conclusions

In this work we undertook a thorough investigation of ground state properties of 1-D quantum gases in a harmonic trap in the presence of a point-like attractive potential. While our analysis makes use of an idealized δ -function potential, it is well known that this approximation encapsulate the basic, qualitative physics of experimentally realistic potentials like focused laser beams or trapped impurities. At these low temperatures, the interaction between a gas and the later one would be particularly well described by a point-like potential.

We have studied both, the many-body properties of a bosonic Tonks-Girardeau and a spin-polarized fermionic gas and calculated the standard many body quantities such as the single particle densities and pair distribution functions. The single particle density was found to be centrally disturbed, in a point-like manner, with effectively no influence on the overall width of the distribution. The pair-distribution function also showed an increase in magnitude for the positions $x, x' = 0$ for increasing potential strength and both these effects could be attributed to the bound eigenstate of the δ -potential.

We have calculated and shown the reduced density matrices for a range of particle numbers and potential strength and, by diagonalisation, were able to derive the the ground state occupation fraction, which is a measure of the coherence inherent in the gas. It was shown that the introduction of the potential to the harmonic trap introduced oscillations in the coherence, with samples consisting of even particle numbers showing larger values. This was confirmed by calculating the experimentally accessible quantities of the momentum distributions and the interference pattern in a time-of-flight experiment.

With results for both, repulsive as well as attractive point potentials, available one can envisage an interesting range of experiments in which the potential strength can be varied as a function of time. For atomic impurities, for example, this would simply correspond to driving the inter impurity-gas scattering length through a Feshbach resonance.

6. Acknowledgements

This project was supported by Science Foundation Ireland under project number 05/IN/I852. D.O'D. has been supported through a UREKA grant 05/IN.1/I852ur07.1. J.G. would like to thank S. McEndoo for enlightening discussions.

References

- [1] I. Bloch, J. Dalibard, W. Zwerger, Rev. Mod. Phys. (in press), arXiv:0704.3011.
- [2] N.H. Dekker, C.S. Lee, V. Lorent, J.H. Thywissen, S.P. Smith, M. Drndic, R.M. Westervelt, and M. Prentiss, Phys. Rev. Lett. **84** 1124 (1999).
- [3] A. Görlitz, J.M. Vogels, A.E. Leanhardt, C. Raman, T.L. Gustavson, J.R. Abo-Shaeer, A.P. Chikkatur, S. Gupta, S. Inouye, T. Rosenband and W. Ketterle, Phys. Rev. Lett. **87**, 130402 (2001).

- [4] H. Ott, J. Fortagh, G. Schlotterbeck, A. Grossmann, and C. Zimmermann, Phys. Rev. Lett. **87**, 230401 (2001).
- [5] R. Dumke, T. Mütther, M. Volk, W. Ertmer, and G. Birkl, Phys. Rev. Lett. **89**, 220402 (2002).
- [6] B.K. Teo and G. Raithel, Phys. Rev. A **65**, 051401(R) (2002).
- [7] K. Günter, T. Stöferle, H. Moritz, M. Köhl, and T. Esslinger Phys. Rev. Lett. **95**, 230401 (2005).
- [8] E.H. Lieb and W. Liniger, Phys. Rev. **130**, 1605 (1963).
- [9] E.H. Lieb, Phys. Rev. **130**, 1616 (1963).
- [10] H. Bethe, Z. Phys. **71**,205 (1931).
- [11] M. Girardeau, J. Math. Phys. **1**, 516 (1960).
- [12] L. Tonks, Phys. Rev. **50**, 955 (1936).
- [13] M. Girardeau, J. Math. Phys. (N.Y.) **1**, 516 (1960); Phys. Rev. **139**, B500 (1965).
- [14] B. Paredes, A. Widera, V. Murg, O. Mandel, S. Fölling, I. Cirac, G.V. Shlyapnikov, T.W. Hänsch and I. Bloch, Nature **429**, 277 (2004).
- [15] T. Kinoshita, T.R. Wenger, D. Weiss, Science **305**, 1125 (2004).
- [16] T. Kinoshita, T. Wenger and D.S. Weiss, Nature **440**, 900 (2006).
- [17] M.D. Girardeau and E.M. Wright, Phys. Rev. Lett. **84**, 5239 (2000).
- [18] M.D. Girardeau , E.M. Wright, and J.M. Triscari, Phys. Rev. A **63**, 033601 (2001).
- [19] T. Busch and G. Huyet, J. Phys. B: At. Mol. Opt. **36**, 2553 (2003).
- [20] Y. Lin and B. Wu, Phys. Rev. A **74**, 013620 (2006).
- [21] Y. Lin and B. Wu, Phys. Rev. A **75**, 023613 (2007).
- [22] J. Goold and Th. Busch, Phys. Rev. A **77**, 063601 (2008).
- [23] X. Yin, Y. Hao, S. Chen and Y. Zhang, arXiv:0804.2759 (2008).
- [24] P. J. Forrester, N.E. Frankel, T.M. Garoni and N.S. Witte, Phys. Rev. A **67**, 043607 (2003).
- [25] T. Papenbrock, Phys. Rev. A **67**, 041601 (2003).
- [26] R. Pezer and H. Buljan, Phys. Rev. Lett. **98**, 240403 (2007).
- [27] D.M. Stamper-Kurn, H.J Miesner, A.P. Chikkatur, S. Inouye, J. Stenger and W. Ketterle, Phys. Rev. Lett. **81**, 2194 (1998).
- [28] T. Weber, J. Herbig, M. Mark, H.C. Nägerl and R.Grimm, Science **299**, 232 (2003).
- [29] H. Uncu, D. Tarhan, E. Demiralp, Ö.E. Müstecaplıoğlu, Phys. Rev. A **76**, 013618 (2007).
- [30] H. Uncu, D. Tarhan, E. Demiralp, Ö.E. Müstecaplıoğlu, Laser Physics **18**, 331 (2008).
- [31] R. Côté, V. Kharchenko, and M.D. Lukin, Phys. Rev. Lett. **89**, 093001 (2002).
- [32] D.S. Murphy, J.F. McCann, J. Goold and Th. Busch, Phys. Rev. A **76**, 053616 (2007).
- [33] M. Olshanii, Phys. Rev. Lett. **81**, 938 (1998).
- [34] K. Huang and C. N. Yang, Phys. Rev. **105**, 767 (1957).
- [35] Th. Busch, B.-G. Englert, K. Rzażewski and M. Wilkens, Found. Phys. **28**, 549 (1998).
- [36] M. Abramowitz and I. Stegun, eds., *Handbook of Mathematical Functions* (Dover, 1972).
- [37] G.J. Lapeyre, J.r., M.D. Girardeau and E.M. Wright Phys. Rev. A **66**, 023606 (2002).